THERMODYNAMIC MODELLING OF THE Al_2O_3-CaO-FeO-Fe_2O_3-PbO-SiO_2-ZnO SYSTEM WITH ADDITION OF K AND NA WITH METALLURGICAL APPLICATIONS

Evgueni Jak & Peter Hayes
The University of Queensland, Australia

Arthur Pelton & Sergei Decterov
École Polytechnique, Canada

ABSTRACT

Computerized thermodynamic databases for the slag and solid oxide phases in the Al_2O_3-CaO-FeO-Fe_2O_3-PbO-SiO_2-ZnO system have been developed by critical evaluation/optimization of all available phase equilibrium and thermodynamic data. The database contains parameters of models for molten slag and solid oxide solutions such as spinel, melilite, olivine, monoxide (wustite, lime), corundum (hematite), etc. The polynomial and sublattice models were used for the solid solutions in this study. The modified quasichemical model was used for the liquid phase. Model parameters are derived by the optimization process to reproduce all thermodynamic and phase equilibrium data within experimental error limits. All binary, ternary and higher order sub-systems were optimised to obtain a self-consistent set of model parameters. This resulted in a significant improvement in the predictive ability of the computer model. The models permit extrapolation into regions of temperature and composition where experimental data are not available. The thermodynamic database is being extended to describe the effects of K and Na oxides – details of the recent thermodynamic optimisation of the Al_2O_3-Na_2O-SiO_2 system are presented.

The thermodynamic databases are automatically accessed by user-friendly FactSage software that calculates complex multi-component multi-phase equilibria involving simultaneously slag, metal, solid and gas phases over wide ranges of temperatures and oxygen partial pressures.

Industrial applications of the databases for the lead / zinc and iron metallurgical processes are discussed.

Key Words: *Thermodynamics, phase equilibrium, phase diagrams, databases, pyrometallurgy, slags, oxide systems.*

INTRODUCTION

Improvements of existing and developments of new high temperature metallurgical and power generation industrial processes require accurate knowledge of the key properties of oxide systems; phase equilibria and thermodynamic properties are of particular importance. Developments of computerised thermodynamic databases supported by extensive experimental investigations with advanced analytical techniques have recently progressed to the level of predicting phase equilibria and other important characteristics for multicomponent multiphase systems close to real industrial chemistries with high accuracy sufficient for practical applications. For example, the FactSage computer package is currently being used extensively around the world in various areas including optimization of bath fluxing and operating temperatures in pyrometallurgical operations, analysis of slagging and fouling during coal combustion and many others. Reliable thermodynamic databases within FactSage are essential for practical applications. The present paper outlines the development of computerized thermodynamic databases for the slag and solid oxide phases in the Al_2O_3-CaO-FeO-Fe_2O_3-PbO-SiO_2-ZnO system with further extension to describe the effects of K and Na oxides. In particular, details of the recent thermodynamic optimisation of the Al_2O_3-Na_2O-SiO_2 system are presented. Industrial applications of the databases for lead/zinc and iron metallurgical processes are discussed.

DEVELOPMENT OF THERMODYNAMIC DATABASES

Thermodynamic databases are developed through thermodynamic optimisation that involves selection of proper thermodynamic models for all phases in a system, critical simultaneous evaluation of all available thermodynamic and phase equilibrium data and optimisation of thermodynamic model parameters to obtain one self-consistent set best reproducing the experimental data as functions of temperature and composition. In the thermodynamic *optimisation* of a system, all available thermodynamic and phase equilibrium data for the system are evaluated simultaneously to obtain one set of model equations for the Gibbs energies of all phases as functions of temperature and composition. From these equations, the thermodynamic properties and the phase diagrams can be back-calculated. Thermodynamic property data, such as activity data, can aid in the evaluation of the phase diagram, and phase diagram measurements can be used to deduce thermodynamic properties. Discrepancies in the available data can be identified during the development of the model. These discrepancies can then be resolved through new experimental studies that, if possible, are undertaken in areas essential for further thermodynamic optimisations. Multicomponent data, if available, are used to derive low-order (binary and ternary) model parameters, and if multicomponent data for a system are lacking, the low-order parameters are extrapolated. In this way, the thermodynamic databases are developed and all the data are rendered self consistent and consistent with thermodynamic principles. The thermodynamic modelling has been carried out using the FactSage computer system [1]. The FACT databases [1] for multicomponent oxide, salt, alloy and aqueous solutions have been developed by critical evaluation/optimization over the last 30 years. The databases contain over 4 400 compounds and 120 non-ideal multicomponent solution phases. The molten slag phase is modelled by the Modified Quasichemical Model [2, 3, 4] in which short-range-ordering is taken into account. Oxide solid solutions are described with a polynomial model or with the Compound Energy Formalism [5], the latter taking into account the crystal structure and physical nature of each solution. For example, the model for spinel [6] describes the distribution of cations and vacancies over tetrahedral (T) and octahedral (O) sites: (Al^{3+}, Fe^{2+}, Fe^{3+}, Zn^{2+})T[Al^{3+},

Fe^{2+}, Fe^{3+}, Zn^{2+}, $Va^{0}]_2{}^{O}O_4$. The olivine solution is modelled by considering two octahedral sites: $[Ca^{2+}, Fe^{2+}, Mg^{2+}, Zn^{2+}]^{M2}(Ca^{2+}, Fe^{2+}, Mg^{2+}, Zn^{2+})^{M1}SiO_4$. The melilite solution is modelled by the mixing of cations on three sublattices $[Ca^{2+}, Pb^{2+}]_2(Fe^{2+}, Zn^{2+}, Al^{3+}, Fe^{3+})[Al^{3+}, Fe^{3+}, Si^{4+}]_2$. Selection of the thermodynamic model for each phase based on the crystal structure ensures high predictive ability of the FACT databases for estimating the properties of multicomponent solutions.

Development of the Database for the Al_2O_3-CaO-FeO-Fe_2O_3-PbO-SiO_2-ZnO System

The multicomponent system Al_2O_3-CaO-FeO-Fe_2O_3-PbO-SiO_2-ZnO has been completely re-optimized by the authors using the new powerful models developed for the liquid slag and multicomponent solid solutions such as spinel, melilite, monoxide, olivine, etc. Parameters of the models have been optimized to represent many thousands of experimental points. All this experimental information from thousands of publications has been critically evaluated, made self-consistent and described with only a few dozen model parameters in the entire oxide database. New models have made it possible to reproduce most experimental data within experimental error limits from 25°C to above the liquidus temperatures at all compositions and oxygen partial pressures from saturation with metals to equilibrium with oxygen.

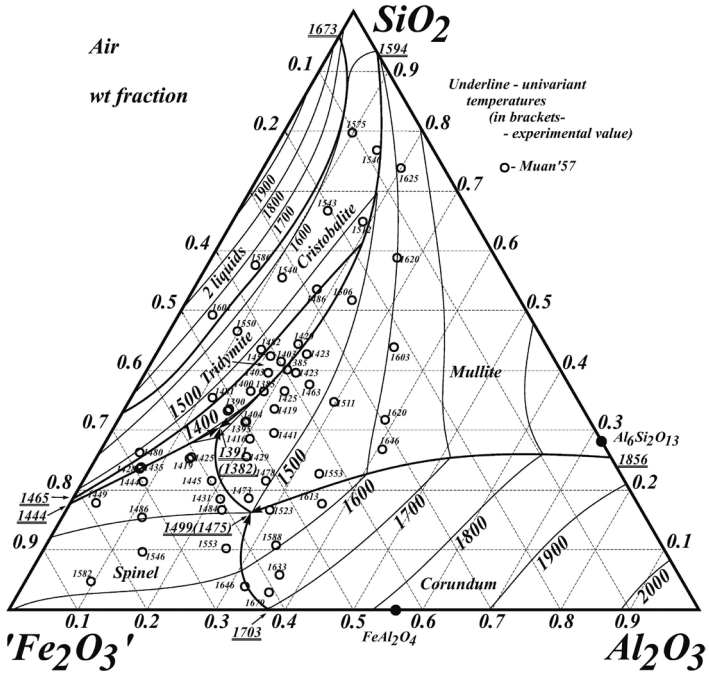

Figure 1: Comparison of predictions to experimental data in the Al_2O_3-'Fe_2O_3'-SiO_2 system in air

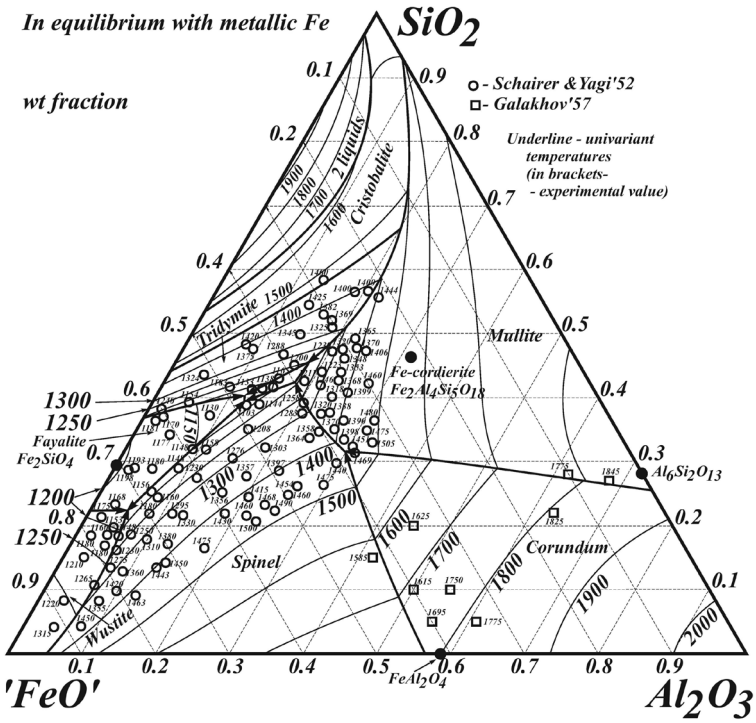

Figure 2: Comparison of predictions to experimental data in the Al_2O_3-'FeO'-SiO_2 system at metallic iron saturation

It is impossible in this short summary to even begin to overview the agreement with all available experimental data used for development of the database. Previous publications presented detailed analyses for some of the lower-order subsystems including Fe-O-Zn [6], Fe-O-Si [7], Fe-O-Si-Zn [8], Fe-O-Pb-Si [9], Ca-O-Pb-Si, [10], Zn-O-Pb-Si [11], Al_2O_3-CaO-SiO_2 [12]. Series of comparisons between predictions and experiments presenting equilibria among major phases in some of the subsystems in the Al_2O_3-CaO-FeO-Fe_2O_3-SiO_2 system over the whole range of oxygen potentials from metal saturation to equilibrium with air are presented by Decterov *et al.* [13]. Many other types of data, including all thermodynamic properties, activities, Fe^{2+}/Fe^{3+} ratios, distributions of cations between different sublattices in solid solutions, partial pressures of equilibrium gaseous species, etc., have also been reproduced and can be calculated and plotted by the software. Further selected comparisons are given in the present paper. Figures 1 and 2 demonstrate the agreement of predictions with the experimental liquidus in the Al_2O_3-FeO-Fe_2O_3-SiO_2 system in air [14] and in equilibrium with metallic iron [15, 16].

In the present work, multicomponent experimental data were generated in parallel to the database development and were used to verify the thermodynamic predictions. In all cases additional iterations from lower-order to multicomponent systems were undertaken to ensure that the models describe simultaneously all available experimental information including the additional experiments in the areas of particular importance to various industrial processes. It is an important aspect of the present work that the thermodynamic modelling is carried out in parallel with an active experimental program so that both studies complement each other. Examples of agreement in such multicomponent systems experimentally investigated and then thermodynamically described by the authors are given in the following figures. Agreement of the predictions

with our recent experimental liquidus measurements in the higher-order system Al-Ca-Fe-O-Si [17] is demonstrated in Figure 3. This is the area of faylite slag that is used in a number of metallurgical processes including Cu smelting slags. Agreement with experiments in the system CaO-FeO-Fe_2O_3-PbO-SiO_2-ZnO [18, 19, 20, 21], important for the lead and zinc pyrometallurgical operations, is demonstrated in Figure 4. Agreement with the experimental liquidus in the Al_2O_3-containing Al_2O_3-CaO-FeO-Fe_2O_3-PbO-SiO_2-ZnO system [22] is demonstrated in Figure 5.

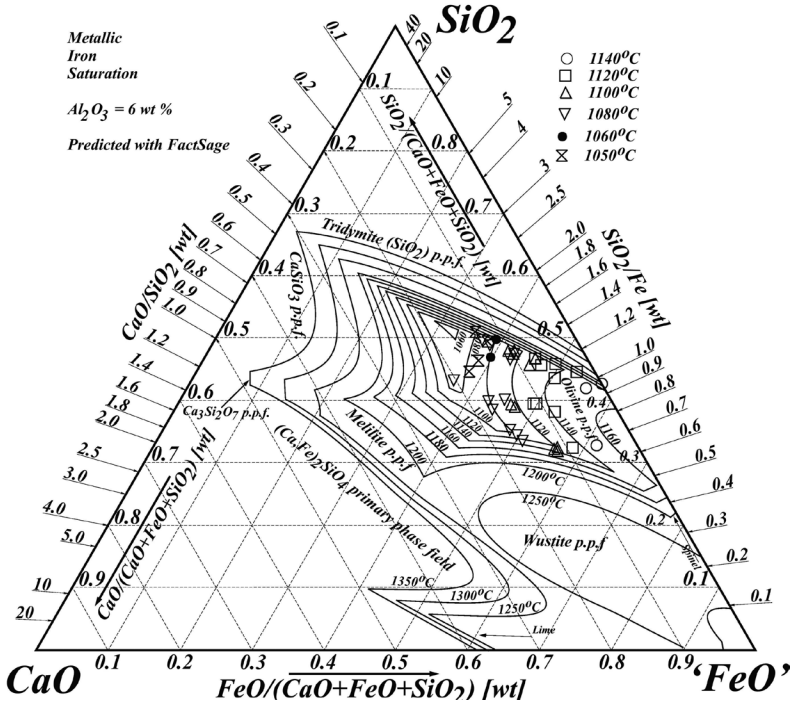

Figure 3: Comparison of predictions to the experimental liquidus in the Al_2O_3-CaO-'FeO'-SiO_2 system at metallic iron saturation and Al_2O_3 = 6 wt%

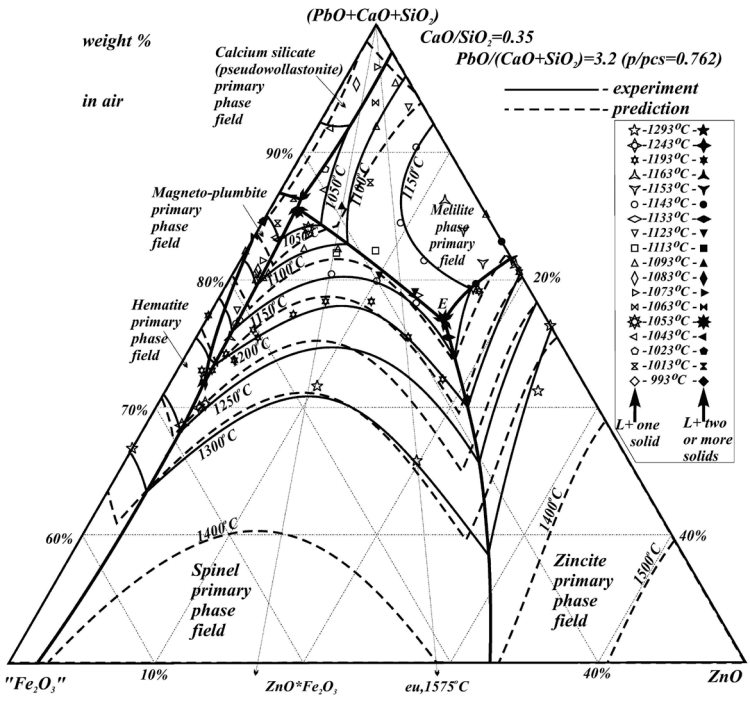

Figure 4: Comparison of predictions to experiments in the ZnO -"Fe_2O_3"- (PbO+CaO+SiO_2) system in air

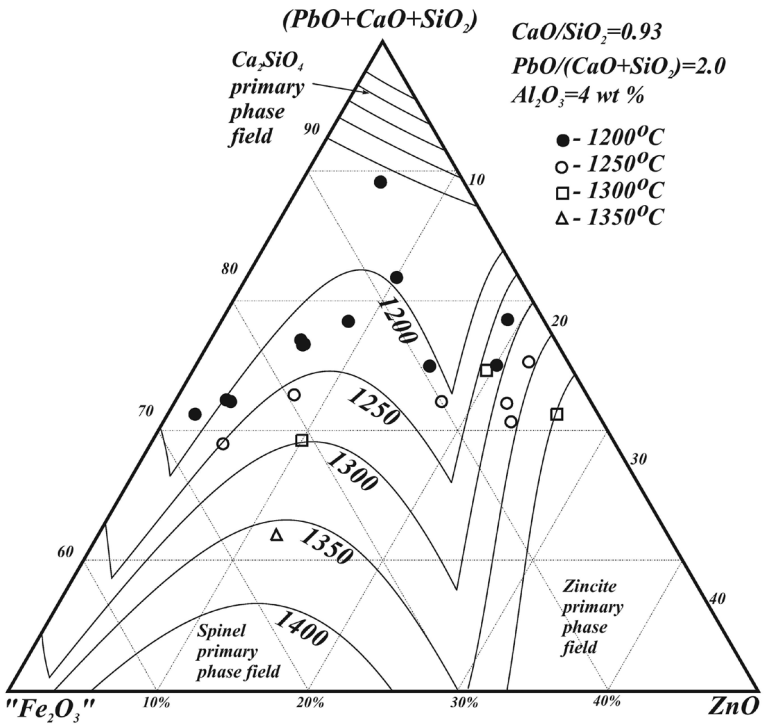

Figure 5: Comparison of predictions to experiments in the Al_2O_3-ZnO-"Fe_2O_3"-(PbO+CaO+SiO_2) system in air

All predictions are consistent with thermodynamic laws and with all available experimental information. The typical scatter of experimental data and the accuracy of model calculations are within experimental error limits for most of the data points. The thermodynamic databases that have been developed make it possible to calculate any other phase diagram sections including regions of composition and temperature where no experimental data are available.

Extension of the Al_2O_3-CaO-FeO-Fe_2O_3-SiO_2 database to describe effects of K and Na

Preliminary thermodynamic optimisations have been performed in the Al_2O_3-CaO-Na_2O-K_2O-FeO-Fe_2O_3-SiO_2 system for all binary, ternary and higher-order subsystems. These are currently being further revised to produce the final self-consistent set of thermodynamic parameters. As part of this work, the Al_2O_3-Na_2O-SiO_2 system has been re-optimised. Figure 6 presents the predicted liquidus surface. All experimental data were described within or nearly within the experimental uncertainties. For example, Figure 7 demonstrates that the experimental liquidus [23, 24, 25] along the $NaAlO_2$-SiO_2 join is well described. No data on solid solutions in the low SiO_2 region at low temperatures were found – continuous solutions between $NaAlO_2$ and nepheline and carnegieite were introduced due to crystal structure similarities. Importantly, all other types of experimental information including heat capacities, enthalpies of formation, heats of mixing, activities, etc have been carefully evaluated and described.

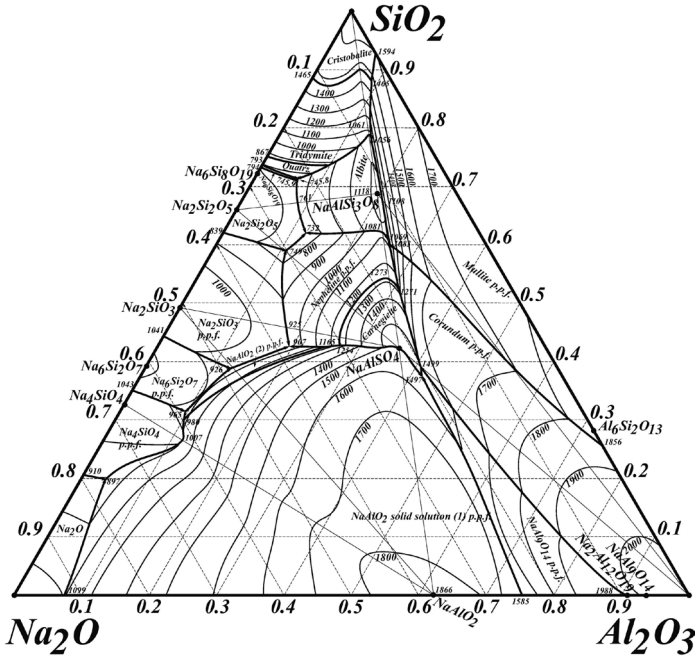

Figure 6: Liquidus in the system Al_2O_3- Na_2O- SiO_2

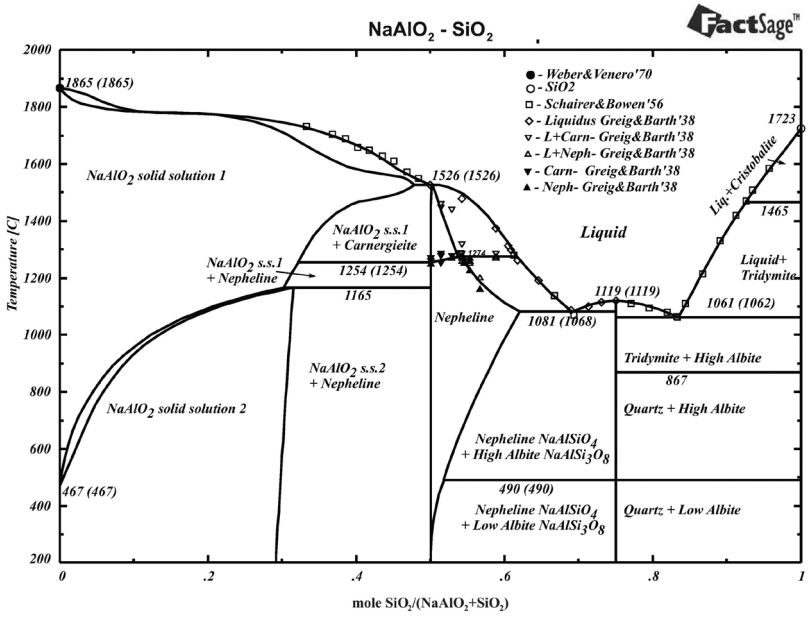

Figure 7: $NaAlO_2$-SiO_2 phase diagram section

For example, Figure 8 shows the agreement between predicted and experimental [26] thermodynamic activities.

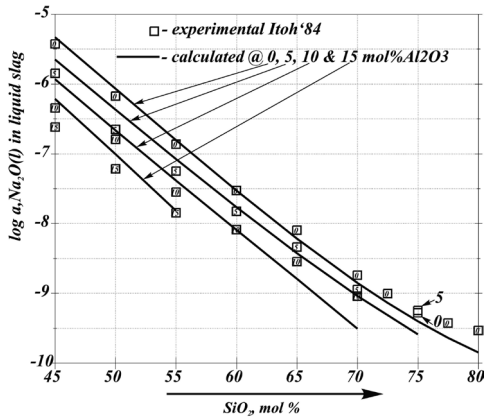

Figure 8: Na_2O activities in the slag phase in the system Al_2O_3-Na_2O-SiO_2

Figure 9 demonstrates the agreement of the predictions with experimental [see ref. 27 to 35] values of enthalpies of crystallisation and enthalpies of mixing of pure liquid oxides in liquid slag solution.

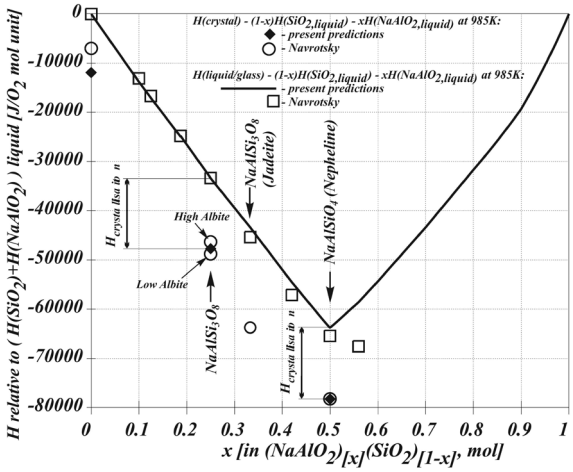

Figure 9: Predicted enthalpy of the liquid slag and solids (quartz, nepheline and albite) relative to the SiO_2+$NaAlO_2$ liquid along the SiO_2-$NaAlO_2$ join compared to experimental data by Navrotsky from solution calorimetry

An essential feature of this system is the strong interaction between Na^+ and Al^{3+} in the oxide melt, usually interpreted as a *charge compensation effect* resulting in the formation of (NaAl) complexes [36]. The thermodynamic modelling of such melts has been proposed previously [37] by the introduction of $(NaAl)^{4+}$ associates as a separate species in the liquid slag solution. This approach was implemented in the present work. Figure 10 illustrates the present predictions of the $(NaAl)^{4+}$ associate concentrations. All three binary subsystems have been optimised either previously (Al_2O_3-SiO_2 [12]) or during the present study. Agreement of the predicted liquidus with experiments in the binary Na_2O-Al_2O_3 [23, 38] and Na_2O-SiO_2 [39, 40, 41, 42] subsystems is demonstrated in Figures 11 and 12 respectively.

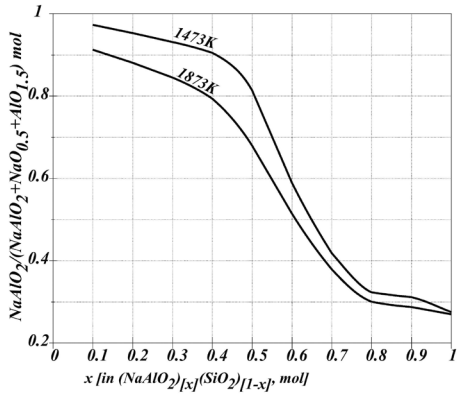

Figure 10: Predicted concentrations of $NaAlO_2$ associates in the liquid slag along the SiO_2-$NaAlO_2$ join

ANALYSIS OF SLAG CHEMISTRY FOR LEAD AND ZINC INDUSTRIAL SLAGS

The potential environmental problems and increasing costs associated with the disposal of zinc-containing wastes has elevated this to an important sustainability issue facing the metallurgical industry. Pyrometallurgical processes are used to produce benign materials for disposal. Improvements of existing and development of new pyrometallurgical processes for these systems are dependent on the detailed analysis of key properties of the slag system. An example of such an analysis is given below. The liquidus, proportions of phases, and Zn and O_2 partial pressures are predicted in the PbO-ZnO-FeO-Fe_2O_3-CaO-SiO_2-Al_2O_3 system in the range of conditions relevant to a selected lead blast furnace slag over a range of compositions (Table 1).

Table 1: Selected conditions

	Average	Range
ZnO	24 wt%	20-30 wt%
Al_2O_3	5 wt %	0 – 8 wt %
FeO/SiO_2	1.27	1.0 – 1.8
CaO/SiO_2	0.71	0.5 – 0.9
Temperature	1200oC	1175-1215°C

A trend analysis has been carried out to systematically determine the effects of changes to the slag chemistry. Of particular interest is the variation in the properties of the system with CaO/SiO_2 and FeO/SiO_2 ratios. Results are presented in the corresponding fluxing diagrams. The phases predicted to be stable in the range of conditions investigated are listed in Table 2 and are indicated with the corresponding name or letter on the diagrams. The liquidus temperatures are presented in Figure 13a. The lead blast furnace slag is close to the boundary between the Wustite and Zincite primary phase fields. According to the predictions, an increase of CaO/SiO_2 ratio at constant FeO/SiO_2 ratio would result in an increase in the liquidus temperatures. Changing FeO/SiO_2 at constant CaO/SiO_2 from the average values would result in an increase in the liquidus temperatures.

Table 2: Phases predicted to be stable in the investigated range

Name	Chemical Formulae	ID
Liquid		L
Wustite	(Fe,Zn)O	W
Spinel	$(Fe,Zn)(Fe^{3+},Al^{3+})_2O_4$	S
Melilite	$(Ca,Pb)_2(Fe^{2+},Zn^{2+})Si_2O_7$	M
Willemite	$(Zn,Fe)_2SiO_4$	D
Zincite	(Zn,Fe)O	Z

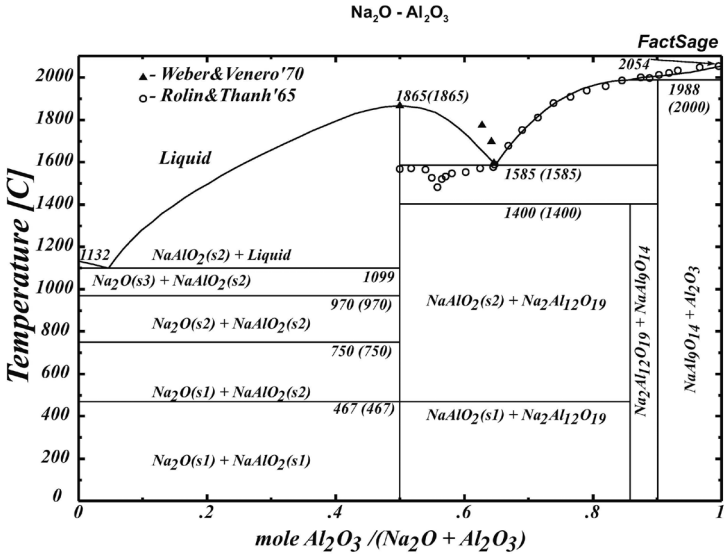

Figure 11: Predicted Al_2O_3-Na_2O phase diagram

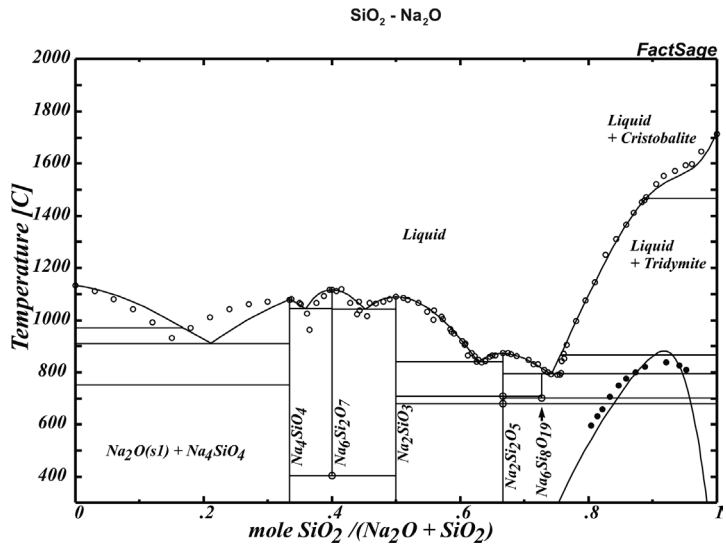

Figure 12: Predicted SiO_2-Na_2O phase diagram compared to experimental data [40, 41, 42, 43]

The proportions of solids at 1200°C (see Figure 13b) are predicted to be insensitive to variations of FeO/SiO_2 or to a decrease of CaO/SiO_2, but increasing CaO/SiO_2 would result in the formation of melilite solid solution in addition to Wustite and Zincite, with an accompanying sharp increase in the proportions of solids. Control of the zinc partial pressures is essential for these Pb/Zn pyrometallurgical operations. The variation of the zinc partial pressure with bulk composition at 1200°C (Figure 13c) is not what might intuitively be expected –P_{Zn} is found to be insensitive to changes in the FeO/SiO_2 ratio, and decreases as the CaO/SiO_2 ratio increases. The main factors effecting P_{Zn} at constant temperature are the activity of ZnO and the oxygen partial pressure P_{O2}. Predictions in this study were made for the condition of a_{Pb}=1 at PbO = 1 wt% in the slag so that, as the bulk

composition changes, both P_{O2} and a_{ZnO} change. Figure 13d shows P_{O2} at 1200°C. It would normally be anticipated that an increase of CaO/SiO_2 would result in an increase of P_{Zn}.

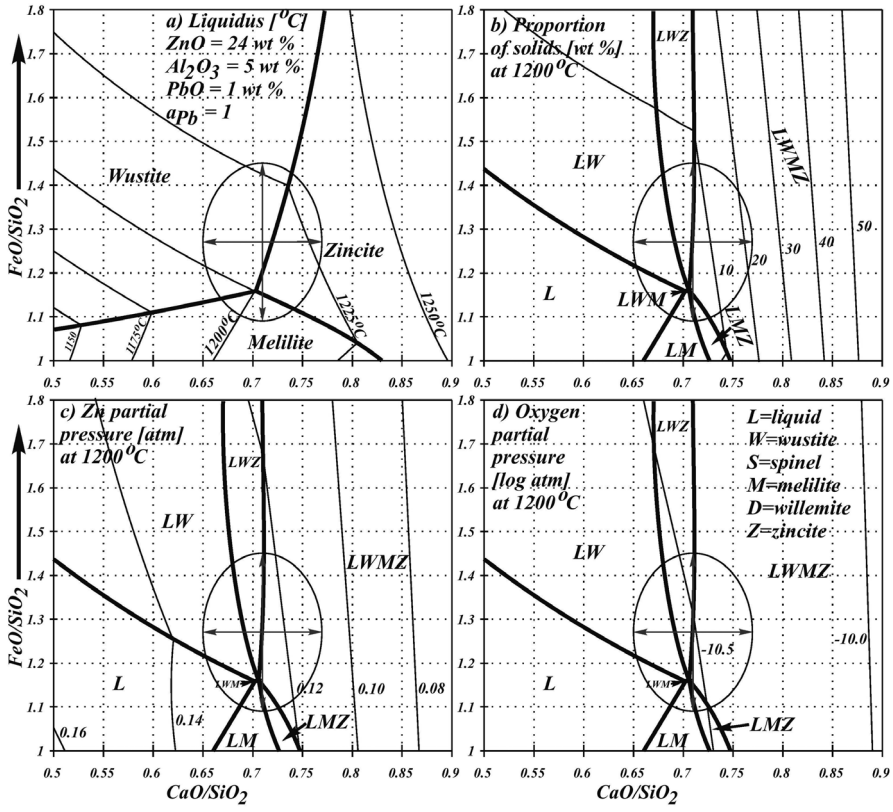

Figure 13: a) Liquidus [°C], b) proportion of solids [wt %], c) Zn partial pressure [atm], and d) Oxygen partial pressure [atm] at 1200°C in a slag system with ZnO = 24 wt%, Al_2O_3 = 5 wt %, PbO = 1 wt% and a_{Pb}= 1

However, a decrease of P_{O2} with an increase of CaO/SiO_2 (see Figure 13d) results in P_{Zn} decreasing. These results provide an important basis for trend analysis of slag behaviour for a lead blast furnace slag to assist with the selection of fluxing and waste recycling.

THE USE OF FactSage TO EXAMINE ALKALI RECIRCULATION IN THE IRON BLAST FURNACE

It is widely recognized that alkali metals can cause operational problems in the iron blast furnace and are strictly controlled. The recently optimized thermodynamic databases describing slags in the system Al_2O_3-CaO-FeO-Fe_2O_3-Na_2O-K_2O-MgO-SiO_2 have been used to predict the behaviour of alkalis in the blast furnace and to examine the effects of changing process variables. The use of these new databases is particularly significant when considering high alkali concentrations and extensive solid solutions that can occur in liquid and solid silicate phases.

The iron blast furnace is a continuous, countercurrent reactor in which oxygen is transferred to the ascending gas phase from the descending ore burden, and heat generated by the combustion of coke is transferred from the ascending gas phase to the descending condensed phases. The furnace is characterized by a thermal and chemical reserve zone in which gas and condensed phases approach equilibrium. In the present study the iron blast furnace is described in terms of a simplified two-step model (see Figure 14) consisting of 1) Hearth Reactor, and 2) Gas Condenser. Coke (stream 2) and preheated air blast (stream 6) enter the Hearth Reactor. Heat loss is indicated as stream 3. Fresh feed (stream 1) reacts with hot gases (stream 7) to form condensed material (stream 9) and heat exchange enthalpy (stream 8), both predicted in the Gas Condenser equilibrium calculations. Streams 7 and 9 enter the Hearth Reactor. Equilibrium calculations for the Hearth Reactor predict output streams including compositions, flow rates and temperature of the slag (stream 4) and liquid iron (stream 5), that leave the Blast Furnace; and composition, flow rate and temperature of the hot gases (stream 7), that are passed into the Gas Condenser. The equilibrium calculation performed for the Gas Condenser predicts the outcomes of a number of reactions including re-oxidation and condensation. Off gases (stream 10) leave the furnace, and condensed material (stream 9) and heat exchange enthalpy (stream 8) are passed into the Hearth Reactor. The calculations are organised in cycles and continued until the mass balance criteria are met, i.e., that the input of volatile elements Na and K in fresh feed (stream 1) equals the Na and K in the output streams including slag (stream 4), iron (stream 5) and off-gases (stream 10) within predetermined values (absolute values differ by less than 0.0005%).

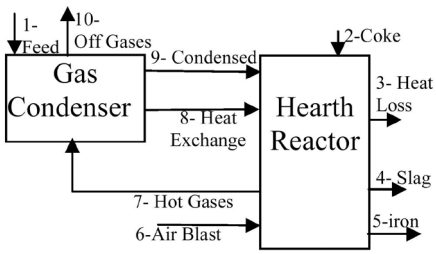

Figure 14: Two-step iron blast furnace model

The FactSage computer package with macros and a new thermodynamic database have been used for phase equilibria predictions of the phases formed and the partitioning of major elements between the solid compounds, liquid oxide, metal and gas phases in the Hearth Reactor and in the Gas Condenser. The model describes heat exchange and associated re-oxidation and condensation reactions in the gas phase during ascent of the gas. The information on the iron blast furnace used for model development includes major feed stream compositions, stream amounts and stream temperatures (see Table 3). The model output includes the compositions, amounts and temperatures of the off-gas, slag, and metal streams. In practice, the total gas pressure within the furnace also changes with height and position.

Table 3: Data on Fukuyama No. 5 furnace [43]

Metal production	**9900 tonnes hot metal (THM)/d**	**Assumtions:**
Hearth diam. HH	14.4 m	• Fe feed is 100% fluxed sinter
Air Blast temp	1550 K	• 50% (SiO_2 + Al_2O_3) impurities in sinter 50% in coke at the same Al_2O_3 /SiO_2 ratios
Hearth temp	1800 K	• All flux materials CaO, MgO and impurities SiO_2, Al_2O_3, Na_2O, K_2O as oxides
Coke rate	470 kg/THM	• S is not considered in the calculations
Air blast	1040 Nm^3/THM	• Hearth Temperature = slag and metal Temp
Slag mass	320 kg/THM	
Alkali load in feed (50% Na_2O /50% K_2O)	10 kg/THM	

Base Slag composition (wt %) ([44], Mannesmann furnace)			
SiO_2	**CaO**	**MgO**	**Al_2O_3**
34.63	41.70	6.74	11.57
Al_2O_3/SiO_2	**CaO/SiO_2**	**Approx.T_{liq}**	
0.334	1.20	1700K	

Table 4: Alkali and alkali earth phases in the Gas Condenser for the base case (No. 2, gas exit 600 K)

Compounds	**t/day**
$K_2Ca_2(CO_3)_3$	3080
$K_2Ca_3Si_6O_{16}$	851
$NaAlSiO_4$, nepheline-b	672
$K_2FeSi_3O_8$	443
KAlSiO, kaliophilite-hexagonal	415
Mg_2SiO_4, forsterite	399
$CaCO_3$, calcite	181

In the present calculations the total pressure is assumed to be 2 atm in the Hearth Reactor and 1 atm in the Gas Condenser, reflecting the pressure drop across the packed bed of the furnace. Table 4 shows a summary of the re-circulating stream - condensed phases predicted to precipitate in the Gas Condenser for the base case. The alkalis in the condenser are predicted to consist principally of solid potassium carbonate and alkali silicate phases. The alkali-containing gas species present in the Hearth Reactor consist predominantly of elemental K and Na, and the cyanides KCN and NaCN. The effects of increasing hearth temperature on alkali recirculation are shown in Figures 15a and 15b; an increase in hearth temperature leads to increased recirculation for both potassium and sodium species. Increasing hearth temperature is accompanied by increasingly positive enthalpies of reaction in the Hearth Reactor and an unfavorable heat balance (Figure 15c). This simplified model of the iron blast furnace demonstrates how important trends in furnace behaviour can be analysed. This is a potentially powerful tool for analysis that can be further extended and refined.

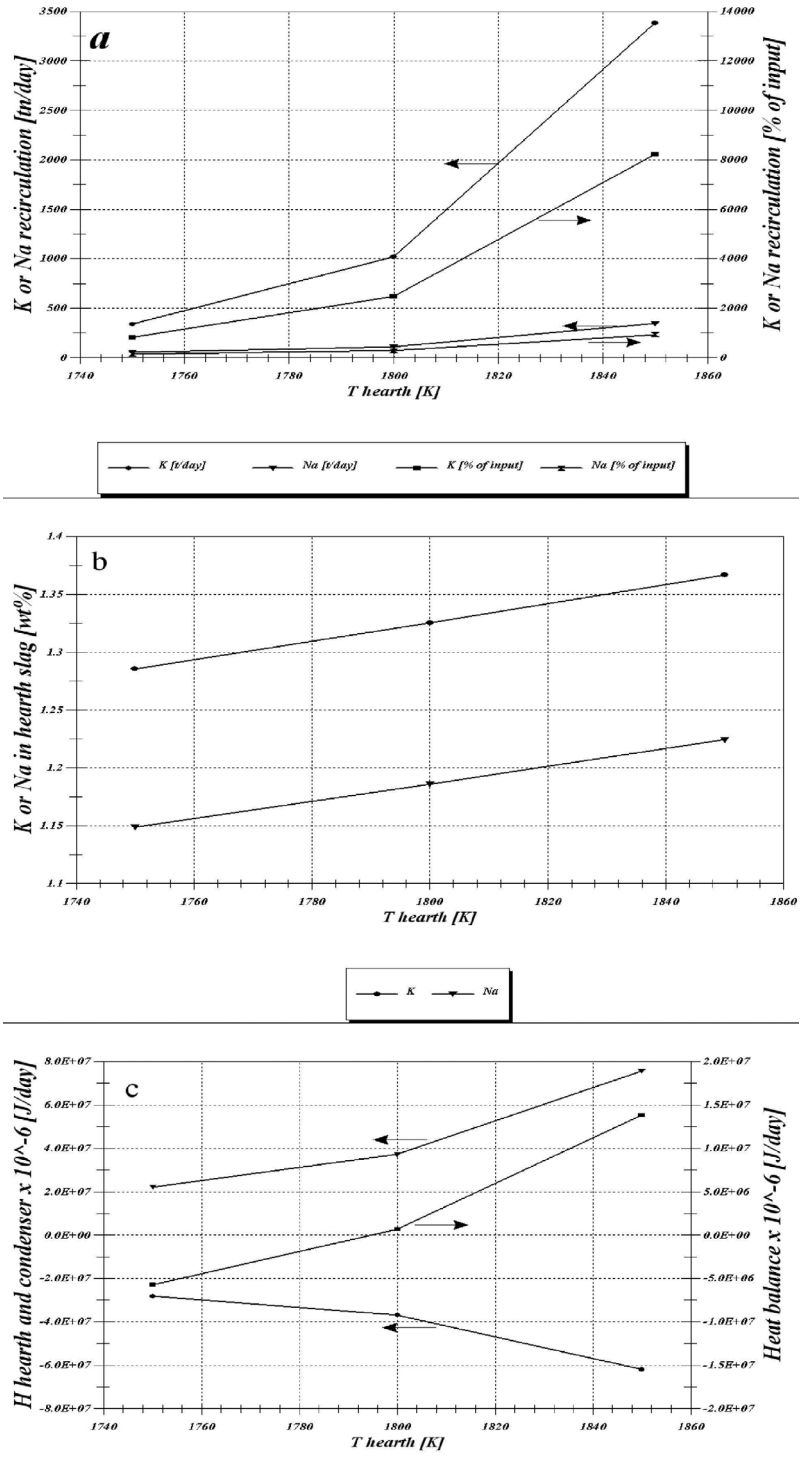

Figures 15: a-c Effects of Fe Blast Furnace hearth temperatures

CONCLUSIONS

Extensive computerized thermodynamic databases have been prepared for solid and liquid oxide phases. These databases have been developed by critical evaluation of all available thermodynamic and phase diagram data through the use of models appropriate to the structure of each solution. The models reproduce all experimental data within experimental error limits and permit good estimations to be made of the thermodynamic properties of multicomponent solutions based on the evaluated and optimized model parameters of lower-order (binary and ternary) subsystems. Modern Gibbs energy minimization software is used to access these databases automatically and calculate the conditions for equilibrium in multicomponent, multiphase systems.

Industrial applications of the databases for the lead/zinc and iron metallurgical processes presented in the paper demonstrate various approaches to the use of this powerful thermodynamic modeling tools.

ACKNOWLEDGMENTS

These database developments have been supported by a number of grants including CRC CCSD, ARC linkage. The authors would also like to thank Nyrstar (formerly Zinifex) Port Pirie and Chris Whitting for support of this work, and permission to publish selected portions of studies of the Pb/Zn slags carried out for the company.

REFERENCES

FactSage. (2008). Ecole Polytechnique, Montréal, http://www.factsage.com/. [1]

Pelton, A. D. & Blander, M. (1986). *Thermodynamic Analysis of Ordered Liquid Solutions by a Modified Quasi-Chemical Approach*. Application to Silicate Slags. Metall. Trans. B, Vol. 17B, pp. 805–815. [2]

Pelton, A. D., Decterov, S. A., Eriksson, G., Robelin, C. & Dessureault, Y. (2000). *The Modified Quasichemical Model. I—Binary Solutions*. Metall. Mater. Trans. B, Vol. 31B. pp. 651–659. [3]

Pelton, A. D. & Chartrand, P. (2001). *The Modified Quasichemical Model. II—Multicomponent Solutions*. Metall. Mater. Trans. A, Vol. 32A. pp. 1355-1360. [4]

Hillert, M., Jansson, B., & Sundman, B. (1988). *Application of the Compound-Energy Model to Oxide Systems*. Z. Metallkd., Vol. 79, No. 2. pp. 81–87. [5]

Decterov, S. A., Jak, E., Hayes, P. C. & Pelton, A.D. (2001). *Experimental Study of Phase Equilibria and Thermodynamic Optimization of the Fe-Zn-O System*. Metall. Mater. Trans.B., 32 B, pp. 643–657. [6]

Jak, E.,Hayes, P., Pelton, A. D., Decterov, S. (2007). Thermodynamic Optimisation of the FeO-Fe_2O_3-SiO_2 (Fe-O-Si) System with FactSage, Gunnar Errikson volume - *International Journal of Materials Research (formerly: Zeitschrift fuer Metallkunde)*, 98(9), 847-854. [7]

Jak, E., Degterov, S. A., Pelton, A. D. & Hayes, P. C. (2001). *Coupled Experimental and Thermodynamic Modelling Study of the System Fe-O-Si-Zn*. Metal. Trans., Vol. 32B, pp. 793-800. [8]

Kudo, M., Jak, E., Hayes, P. C., Yamaguchi, K. & Takeda, Y. (2000). *Lead Solubility in FeO_x-CaO-SiO_2 Slags at Iron Saturation*. Metal.Trans., Vol. 31B, pp. 15-24. [9]

Jak, E., Degterov, S., Hayes, P. C. & Pelton, A. D. (1998). *Thermodynamic Optimisation of the Systems CaO-Pb-O and PbO-CaO-SiO_2, Can*. Metal. Quart., Vol. 37 (1), pp. 41-47. [10]

Jak, E., Degterov, S., Wu, P., Hayes, P.C. & Pelton A.D. (1997). *Thermodynamic Optimisation of the Systems PbO-SiO_2, PbO-ZnO, ZnO-SiO_2 and PbO-ZnO-SiO_2*. Metal.Trans., vol. 28B, pp. 1011 1018. [11]

Eriksson, G. & Pelton, A. D. (1993). *Critical Evaluation and Optimization of the Thermodynamic Properties and Phase Diagrams of the CaO-Al_2O_3,Al_2O_3-SiO_2 and CaO-Al_2O_3-SiO_2 Systems*. Met.Trans,24B, 807–816. [12]

Decterov, S., Jung, I. H., Jak, E., Hayes, P., & Pelton, D. (2004). *Thermodynamic Modeling of the Al_2O_3-CaO-CrO-Cr_2O_3-FeO-Fe_2O_3-MgO-MnO-SiO_2-S System and Applications in Ferrous Process Metallurgy*. VII Int.Conf. on Molten Slags, Fluxes and Salts, Capetown, publ. The South African Inst. Of Mining and Metallurgy, Johannesburg, South Africa, ISBN 1-919783-58X, pp. 839-850. [13]

Muan, A. (1957). Phase Equilibria at Liquidus Temperatures in the System Iron Oxide-Al_2O_3-SiO_2 in Air Atmosphere, *Journal of the America Ceramic Society*, Vol. 40, p. 127. [14]

Schairer, J. F. & Yagi, K. (1952).*The System FeO-Al_2O_3-SiO_2*. Am.J.Sci. Vol. Part 2, pp. 471-512. [15]

Galakhov, F. Ya. (1957). *Izv. Akad.Nauk SSSR*. Otdel Khim.Nauk, Vol. 5, pp. 525-531. [16]

Zhao B., Jak E. & Hayes P. C. (1999). *The Effect of Al_2O_3 on Liquidus Temperatures of Fayalite Slags*. Metal.Trans., Vol. 30B, pp. 597-605. [17]

Jak E. & Hayes P. (2002). *Experimental Lliquidus in the PbO-ZnO-"Fe_2O_3"-(CaO+SiO_2) System in Air with CaO/SiO_2 = 0.35 and PbO/(CaO/SiO_2) = 3.2*. Met.Trans B, Vol. 33B, pp. 851-863. [18]

Jak, E. & Hayes, P. (2002). *Experimental Study of Phase Equilibria in the PbO-ZnO-"Fe_2O_3"-(CaO+SiO_2) System in Air for High Lead Smelting Slags (CaO/SiO_2 Weight Ratio of 0.35 and PbO/(CaO/SiO_2) Ratio of 5.0)*. Met.Trans B, Vol. 33B, pp. 817-825. [19]

Jak, E. & Hayes, P. (2003). *The Effect of the CaO/SiO_2 Ratio on the Phase Equilibria in the ZnO-"Fe_2O_3"-(PbO+CaO+SiO_2) System in Air; CaO/SiO_2=0.1, PbO/(CaO/SiO_2) = 6.2 ; and CaO/SiO_2= 0.6, PbO/(CaO/SiO_2) = 4.3)*, Met.Trans B, Vol. 34B, pp. 369-382. [20]

Jak, E., Zhao, B., Harvey, I., & Hayes, P. (2003). *Experimental Study of Phase Equilibria in the PbO-ZnO-"Fe_2O_3"-(CaO+SiO_2) System in Air for the Lead and Zinc Blast Furnace Sinters (CaO/SiO_2 Weight Ratio of 0.933 and PbO/(CaO/SiO_2) Ratios of 2.0 and 3.2)*. Met.Trans B, Vol. 34B, pp. 383-397. [21]

Chen, S., Zhao, B., Hayes, P.C. & Jak E. (2001). *Experimental Study of the System 4%Al_2O_3 + ZnO-"Fe_2O_3"–(PbO+CaO+SiO_2), CaO/SiO_2 =0.93 and PbO/(CaO+SiO_2)=2.0 in Air, Pyrometallurgy Research Centre*. The University of Queensland, http://pyrosearch.minmet.uq.edu.au/, Private Communications. [22]

Weber, N. & Venero, A. F. (1970). 72nd Ann.Meet.Am.Ceram.Soc., Philadelphia 5-JI-70, Vol. 7, pp. 141. [23]

Schairer, J. F. & Bowen, N. L. (1856). Am J Sci ,Vol. 254 (731), pp. 129-204. [24]

Greig, J. W. & Barth, T. F. W. (1938). Am J Sci , Vol. 35A (5), pp. 94. [25]

Itoh, H. & Yokokawa, T. (1984). *Thermodynamic Activity of Na_2O in Na_2O-SiO_2-Al_2O_3 Melt*. Trans. Jap. Inst. Metals, Vol. 25, pp. 879-884. [26]

Navrotsky, A., Hervig, R., Rot, B. N., & Huffman, M. (1985). High Temperature Sci., Vol. 19, pp. 133-150. [27]

Carpenter, M., McConnel, J. & Navrotsky, A. (1985). Geochim.et Cosmochim.Acta, Vol. 49, pp. 947-966. [28]

Navrotsky, A., Peraudeau, G., McMillan, P., & Coutures, J. P. (1982). Geochimica et Cosmochimica Acta, Vol. 46, pp. 2039-2047. [29]

Navrotsky, A., Hon, R., Weill, D. F. & Henry D. J. (1980). Geochim. Cosmochim. Acta, 44(10), pp. 1409-1423. [30]

De Yoreo, J. J., Navrotsky, A., & Dingwell, D. B. (1990). J. Am. Ceram. Soc. Vol. 73, pp. 2068-2072. [31]

Roy, B. N. & Navrotsky, A. (1984). J.Amer.Ceram.Soc. Vol. 67, pp. 606-610. [32]

Weill, D. F., Hon, R., & Navrotsky, A. (1980). Phys. Magmat. Processes, Proc., Vol. pp. 49-92. [33]

Navrotsky, A., Capobianco, C., & Stebbins, J. (1982). J.Geol., Vol. 90(6), pp. 679-98. [34]

Petrovic, Ivan & Navrotsky, A. (1997). Microporous Mater. vol. 9(1,2), pp. 1-12. [35]

Stebbins, J. F., McMillan, P. F. & Dingwell, D. B. (1995). *Structure, Dynamics and Properties of Silicate Melts*. Reviews in Mineralogy., Publ.: Mineral. Soc.of America, Washington, D. C., 616 pp. [36]

Chartrand, P. & Pelton, A. D. (1999). *Modeling the Charge Compensation Effect in Silica-Rich Na_2O- K_2O-Al_2O_3-SiO_2 Melts*. Calphad, 23(2), pp. 219-230. [37]

Rolin, M. E & Thanh, P. H. (1965). *Les Diagrammes de Phases des Melanges ne Reagissant pas avec le Molybdene*. Rev. Hautes Temp. Refractaires, Vol. 2, pp. 175-185. [38]

Morey, G. W. & Bowen, N. L. (1924). *The Binary System Sodium Metasilicate-silica*. J Phys. Chem. Vol. 28, pp. 1167-79. [39]

Kracek F. C. J. (1930). *The System Sodium Oxide-Silica*. Phys.Chem.(Am Ceram Soc), 34, 1583-1598. [40]

Schairer, J. F. & Yoder, Jr. H. S. (1969-1970). *The Compound $3Na_2O*8SiO_2$ in the System Na_2O*SiO_2*. Carnegie Institution of Washingtoon, year book 69, Vol. pp. 160-163. [41]

Kracek, F. C. (1930). J Am Ceram. Soc. Vol. 52, pp. 1440. [42]

Peacey, J. G. & Davenport ,W. G. (1979). *The Iron Blast Furnace – Theory and Practice*. Pergamon. [43]

Biswas, A. K. (1981). *Principles of Blast Furnace Ironmaking – Theory and Practice*. SBA Publications, Calcutta, India. [44]